frontiers | Frontiers in Forests and Global Change

TYPE Original Research
PUBLISHED 15 January 2026
DOI 10.3389/ffgc.2025.1743125

OPEN ACCESS

EDITED BY
Avram Sorin,
University of Craiova, Romania

REVIEWED BY
Mihaita Iulian Niculae,
University of Bucharest, Romania
Alexandru Sin-Schneider,
National Institute for Economic Research (NIER), Romania

*CORRESPONDENCE
Xia Yu
✉ xiayuyn@163.com

RECEIVED 10 November 2025
REVISED 18 December 2025
ACCEPTED 18 December 2025
PUBLISHED 15 January 2026

CITATION
Li H, Xu J, Ning C and Yu X (2026) Quantifying the spatiotemporal dynamics of net primary productivity under climate change using MOD17A3 NPP product and meteorological reanalysis datasets in the Yihe River Basin, East China (2001–2023). *Front. For. Glob. Change* 8:1743125. doi: 10.3389/ffgc.2025.1743125

Quantifying the spatiotemporal dynamics of net primary productivity under climate change using MOD17A3 NPP product and meteorological reanalysis datasets in the Yihe River Basin, East China (2001–2023)

Hongyuan Li[1,2], Jingru Xu[3], Chuanchuan Ning[1] and Xia Yu[4]*

[1]School of Resources and Environment, Linyi University, Linyi, China, [2]Qilian Alpine Ecology and Hydrology Research Station, Northwest Institute of Eco-Environment and Resources, Chinese Academy of Sciences, Lanzhou, China, [3]Kaiyuan Middle School, Laoling, China, [4]Linyi People's Hospital, Linyi, China

Accurately assessing regional ecological sustainability and responses to climate change requires clarifying the spatiotemporal dynamics of Net Primary Productivity (NPP), a fundamental and climate-sensitive indicator of ecosystem structure and carbon sequestration. To clarify the spatiotemporal dynamics of NPP under climate change and provide insights for regional ecosystem management and policy formulation, this study employed trend and correlation analysis methods to quantify the spatiotemporal variations in NPP and their relationship with climate change in the Yihe River Basin (YRB), a typical warm temperate monsoon basin in East China with complex topography and diverse land use, based on MOD17A3HGF data and meteorological reanalysis datasets during 2001 and 2023. The results indicate that: (1) NPP within the basin exhibits fluctuating yet overall increasing trends, with declines predominantly observed in urban and adjacent areas; (2) The multi-year average of annual total NPP in the basin was 20.24 TgC, the multi-year average of annual mean NPP was 403.75 gC/m^2/a, and the spatial distribution showed significant heterogeneity, with higher values in mountainous peripheral areas and lower values in urbanized central zones; (3) Both temperature and precipitation within the basin exhibit upward trends, with precipitation identified as the primary climatic factor positively correlated with NPP, suggesting it may be the key driver of NPP increase. This study confirms the dominant role of precipitation in regulating NPP dynamics in warm temperate monsoon basins, providing a scientific basis for climate adaptation and ecological management in the YRB and similar regions globally.

KEYWORDS

net primary productivity, spatiotemporal dynamics, precipitation, climate change, Yihe River Basin

1 Introduction

Against the backdrop of global climate change, the average global surface temperature has risen by approximately 1.1 °C since the pre-industrial period, with frequent occurrences of extreme climate events such as heatwaves, droughts, and heavy precipitation, posing severe challenges to the stability and service functions of terrestrial ecosystems (IPCC, 2021). As the largest carbon pool and core component of the Earth system, terrestrial ecosystems play a pivotal role in regulating global carbon cycling, mitigating climate change, and maintaining biodiversity (FAO, 2023; IPCC, 2022). Understanding the response mechanisms of terrestrial ecosystems to environmental variations has thus become a core issue in global ecological research and climate governance. Net Primary Productivity (NPP), defined as the organic carbon accumulated by green plants through photosynthesis minus carbon loss via autotrophic respiration, is not only a key indicator reflecting terrestrial ecosystem structure integrity, carbon sequestration capacity, and functional stability but also a critical link connecting vegetation growth, carbon cycling, and climate regulation services (Running et al., 2004; Field et al., 1998). It represents the net carbon available for plant growth and energy flow across trophic levels, serving as a fundamental basis for crucial ecosystem services in terms of climate regulation, soil conservation, and biomass production (Ma et al., 2024). Beyond ecological research, NPP also quantifies the capacity of terrestrial ecosystems to serve as carbon sinks, mitigating rising atmospheric CO_2 concentrations (IPCC, 2021). The high sensitivity of NPP dynamics to both climatic factors and human activities offers a critical perspective for understanding the mechanisms by which ecosystems respond to environmental change (Wang Y. et al., 2025; Zhao H. et al., 2025; Long et al., 2024; Yuan et al., 2023; Chen et al., 2020; Wu et al., 2014), it has become an essential metric for assessing ecosystem health and resilience (Gu et al., 2025; Zhao H. et al., 2025; Han et al., 2024), thereby providing a scientific basis for climate policy and sustainable development strategies. Therefore, quantifying the spatiotemporal dynamics of NPP and its driving mechanisms is not only essential for improving the accuracy of global climate change predictions but also provides a scientific basis for formulating targeted climate adaptation strategies and sustainable development policies at regional and global scales.

With the widespread application of ground-based observations, ecological models, and remote sensing technologies in recent decades, extensive monitoring and simulation studies on changes in NPP have been conducted globally (Cong et al., 2025; Du et al., 2025; Song et al., 2025; Zhu et al., 2023; Gang et al., 2017; Lin and Dugarsuren, 2015; Yan et al., 2015; Pachavo and Murwira, 2014). These studies demonstrate that climatic factors such as solar radiation, temperature, and precipitation, alongside human activities including land use change and ecological policies, collectively shape the spatiotemporal distribution patterns of NPP across different ecosystems (Li et al., 2023; Gang et al., 2017). At global and regional scales, most studies indicate an overall increasing trend in terrestrial NPP in recent decades, albeit with significant spatial heterogeneity. For instance, Tum et al. (2016) estimated a global NPP increase at a rate of approximately 0.04 PgC/a, while regional analyses reveal variations driven by climate variability, rising atmospheric CO_2 concentrations, and human land use activities. Across global regions, these regional variations manifest as distinct patterns of NPP change and underlying driving mechanisms, as documented in existing studies: For instance, the average NPP of forests in Romania reaches 6.38 TC/ha/a, with nearly 99% of forested areas exhibiting a significant positive trend, where temperature serves as the primary climatic driver of this growth (Prăvălie et al., 2023). In contrast, forest and shrub vegetation in southwestern Australia, a typical Mediterranean climate zone which shows a marked decreasing NPP trend, primarily attributed to reduced annual precipitation and increased frequency of extreme drought events (Brouwers and Coops, 2016). Similarly, India's NPP displays a slight overall increasing trend with notable spatial heterogeneity, and precipitation acts as the dominant controlling factor for NPP in 72% of the region (Bejagam and Sharma, 2022). Meanwhile, in the savannas of Southern Africa, NPP is significantly positively correlated with both shortwave radiation and precipitation, with these two factors jointly driving variations in regional vegetation productivity (Pachavo and Murwira, 2014). Additionally, in south-central Chile, exotic tree plantations boast significantly higher NPP-derived exergy due to intensive forest management, though their expansion has concurrently caused ecological fragmentation and biodiversity loss (Martínez et al., 2019).

In China, large-scale government-led ecological restoration projects, such as the Natural Forest Protection Program (NFPP) and the Grain-for-Green Program (GFGP), have significantly enhanced vegetation coverage and productivity (Gong et al., 2023; Yang et al., 2014). For instance, Li et al. (2023) reported a significant increasing trend in NPP across the Loess Plateau between 2000 and 2020, with climate change and human activities contributing approximately 62% and 38% of the increase, respectively. Meanwhile, NPP dynamics in the Yangtze River Basin show a strong correlation with precipitation patterns (Yang et al., 2021). Similarly, Chen et al. (2020) found in their study of southern China that afforestation significantly increased the Leaf Area Index as well as NPP, though its longer-term sustainability faces challenges from water constraints and biodiversity loss. Notably, the effectiveness of these ecological projects exhibits significant regional heterogeneity owing to diverse climatic conditions, intensity of human intervention, and differences in vegetation types. Furthermore, the beneficial effects of ecological restoration are often partially offset by rapid urbanization and concomitant socio-economic development, particularly in highly developed regions like the Yangtze River Delta (Wu et al., 2014) as well as the Beijing-Tianjin-Hebei region (Zhang et al., 2024). Work by these authors highlights that assessing regional NPP dynamics is indispensable for contextualizing its role under global change.

Therefore, accurately assessing regional NPP dynamics is crucial for understanding ecosystem responses and adaptations under global change. Against this context, delving into the driving mechanisms behind the spatiotemporal dynamics of NPP is particularly important. Research indicates that, constrained by local climatic conditions, different ecosystem types exhibit varying NPP responses to climate change (Gang et al., 2017). In water-limited ecosystems, such as arid regions, semi-arid grasslands and the Loess Plateau, precipitation is the primary factor driving interannual variability in NPP (Zhou et al., 2025; Xu et al., 2024; Yan et al., 2016). Conversely, in temperature-limited systems, including the Qinghai-Tibet Plateau and boreal coniferous forests, thermal conditions, particularly growing season temperatures, constitute the primary constraints on vegetation growth (Liang et al., 2024; Tang et al., 2024). Additionally, rising atmospheric CO_2 concentrations enhance photosynthesis through the CO_2 fertilization effect, contributing significantly to the global NPP increase, such as Hu et al. (2024) estimated this effect accounts for approximately 32% of the observed change. However, complex interactions exist among these climatic drivers; for example, warming may prolong the growing season in cold regions while potentially exacerbating water stress in arid areas (Wang F. et al., 2025; Xue et al., 2023).

Advances in observation technology, particularly the widespread application of remote sensing products such as the MODIS NPP datasets, has greatly facilitated large-scale, long-term monitoring of vegetation dynamics (Liu et al., 2025; Tang et al., 2024; Wang et al., 2023; Xi et al., 2023; Zhu et al., 2023). Coupled with high-resolution meteorological reanalysis data, these datasets enable robust spatiotemporal analysis and driving mechanism identification. For instance, studies based on remote sensing techniques in the Yellow River Basin (Wang et al., 2024; Chen et al., 2023), the Heihe River Basin (Yan et al., 2016), and the Three-North Shelter Forest Program Area (Gong et al., 2023), have not only revealed the spatiotemporal dynamics of NPP but also successfully identified the corresponding impacts of climate change as well as human activities to its variations, highlighting the importance of water resource availabilities in arid and semi-arid regions, which alongside the significance of temperature or radiation for the humid areas. Beyond remote sensing techniques, other advanced statistical methods including geographical detector, residual trend analysis, and machine learning algorithms have also played a crucial role in identifying dominant factors and their interactions (Wang et al., 2023; Xue et al., 2023).

River basins, serving as integrated hydrological and ecological units, provide an ideal scale for comprehensively understanding ecosystem dynamics. While studies on major Chinese river basins, notably the Yellow (Chen et al., 2023) and Yangtze Rivers (Yang et al., 2021), have revealed distinct NPP patterns and driver-response relationships, research on medium-scale basins like the Yihe River Basin (YRB) remains relatively scarce, representing a critical gap in regional carbon cycle studies. The YRB, the largest tributary of the Huaihe River system, is located in southeastern Shandong Province, East China, and represents a typical temperate monsoon climate zone. As an important ecological barrier and agricultural production base in East China, the YRB faces the dual pressures of climate change and intensive human activities. Specifically, the spatiotemporal dynamics of NPP in the YRB and its response mechanisms to climate change remain unclear, limiting the scientific formulation of regional ecological management policies. Addressing this issue is necessarily for coordinating ecological conservation and socio-economic development in the basin and similar temperate monsoon regions.

Therefore, in order to deepen understanding of carbon cycling processes, providing scientific basis for regional ecological restoration and climate change adaptation, the present study quantified the spatiotemporal dynamics of NPP in the YRB under climate change, utilizing MOD17A3HGF NPP data alongside high-resolution meteorological reanalysis datasets spanning 2001–2023. Specific objectives include: (1) quantifying the temporal evolution trends and spatial distribution patterns of NPP; (2) revealing the impact of climate change on variations in NPP; and (3) proposing targeted ecological management strategies and climate adaptation recommendations for the basin based on research findings.

2 Materials and methods

2.1 Study area

The YRB constitutes a critical ecosystem within the temperate monsoon climate zone of East China (Figure 1). Geographically, the Yihe river originates in the mountainous Yimeng region of south-central Shandong Province, flowing southward into Jiangsu Province before discharging into the Yellow Sea. This study defines the catchment area upstream of the Linyi Hydrological Station as the study area, encompassing a total area of approximately 10,462 km^2. Administratively, it includes most of Yiyuan (YY), Yishui (YS), Mengyin (MY), Yi'nan (YN), Pingyi (PY), and Fei (FX) counties, along with parts of Lanshan (LS) District.

The basin's topography is complex and varied, predominantly characterized by hills and mountains, with a general slope dipping from the northwest to the southeast. Climatically, it exhibits a typical temperate monsoon climate with distinct seasons, abundant sunshine, and highly uneven precipitation distribution. The annual precipitation averages between 700 and 900 mm, with 65%–70% concentrated during June and September as intense, episodic extreme rainfall events (Liu, 2020). Conversely, winters are dry, and spring frequently experiences drought conditions, leading to significant interannual runoff variability. To manage water resources, major reservoirs such as the Bashan Dam and Andi Dam have been constructed within the basin. In terms of land use (Figure 2), cropland predominates, accounting for over 62% of the basin, while urban construction land and forested land constitute 17% and 12%, respectively (Qiao et al., 2025). Over the past two decades, urban expansion has steadily reduced cropland proportion, accompanied by increased impervious surfaces that adversely affect ecological and hydrological processes (Yang and Li, 2024). The basin's vegetation types include agricultural ecosystems (winter wheat, maize, peanuts) and deciduous broadleaf forests, with mountainous areas renowned for fruits such as apples, peaches, and chestnuts (LBS, 2024).

Ecologically, the basin exhibits marked spatial heterogeneity: upstream mountainous regions boast relatively high vegetation coverage and rich biodiversity, protected within areas like the Yimeng Mountain National Geopark and the Lu Mountain Provincial Nature Reserve. In contrast, midstream and downstream areas suffer from lower vegetation coverage, exacerbated by increasing pressures from agricultural and industrial activities, which have led to significant water pollution (Li, 2025). Consequently, despite its cultural and economic value, the basin faces multiple ecological challenges, including water scarcity, uneven water distribution, water pollution, soil erosion, and ecological degradation, rendering its ecosystem relatively fragile (Qiao et al., 2024). This combination of climatic sensitivity, pronounced human influence, and spatial ecological variability makes the YRB a region of critical importance for investigating the spatiotemporal dynamics of climate change impacts on NPP.

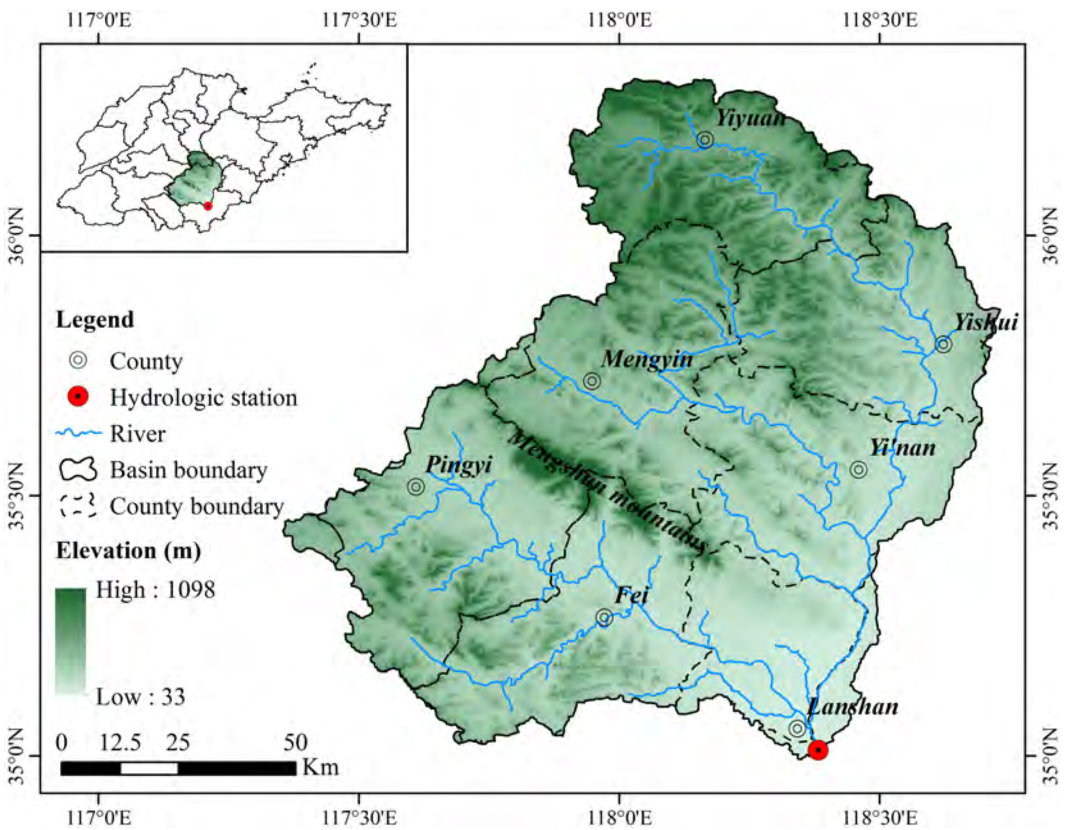

FIGURE 1
Geographical location and overview of the Yihe River Basin (YRB).

2.2 Data

2.2.1 NPP data

The annual mean NPP data employed in this study originates from the MOD17A3HGF Version 6 product from the NASA MODIS datasets (Running and Zhao, 2019). This dataset provides global annual NPP estimates at a spatial resolution of 500 meters, representing the net amount of carbon sequestered by vegetation after accounting for respiratory losses. The data span the period from 2001 to 2023 and are projected using the WGS_1984_Albers coordinate system. Each pixel's NPP value is scaled by 0.0001 to obtain actual units, and quality control (QC) bands are included to filter unreliable pixels due to cloud contamination or sensor errors. The MOD17A3HGF product addresses known issues in cloud-related inaccuracies in LAI-FPAR inputs and is widely validated for ecological studies (Hu et al., 2024; Running and Zhao, 2019).

2.2.2 Meteorological reanalysis data

Meteorological reanalysis data, including reanalyzed monthly mean temperature (T_a) and monthly precipitation (*Pre*), were accessed at the National Tibetan Plateau Data Center (Peng, 2020, 2019). This dataset, developed by Peng et al. (2019), offers high-resolution 1,000 m gridded data for China, with temperature and precipitation data accuracy of 0.1 °C and 0.1 mm, respectively. The data span from 1901 to 2024 and were generated through a delta spatial downscaling approach, integrating CRU global climate data and WorldClim high-resolution datasets, validated against observed temperature and precipitation from nearly 500 independent standard meteorological stations across China. Stored in NETCDF format (*.nc), this dataset is widely recognized for its applicability in climate-change-related research due to its long-term coverage and spatial consistency.

2.2.3 Data preprocessing

To ensure spatial consistency, the NPP data and meteorological reanalysis data were projected to one uniformly coordinate system of the WGS_1984_Albers. The meteorological reanalysis data, originally at a 1,000 m resolution, were downscaled to 500 m using bilinear interpolation-based resampling method to match the spatial resolution of the NPP data. Monthly temperature and precipitation values were aggregated to annual means and totals, respectively, to match the temporal resolution of NPP. Both datasets were clipped to the spatial extent of the YRB using a boundary shapefile and converted into the GeoTIFF format for compatibility with GIS software, enabling pixel-level analysis of correlations between NPP and climatic factors.

2.3 Methods

2.3.1 Trend analysis

In studies quantifying the evolutionary characteristics of variables over time, trend analysis serves as a fundamental

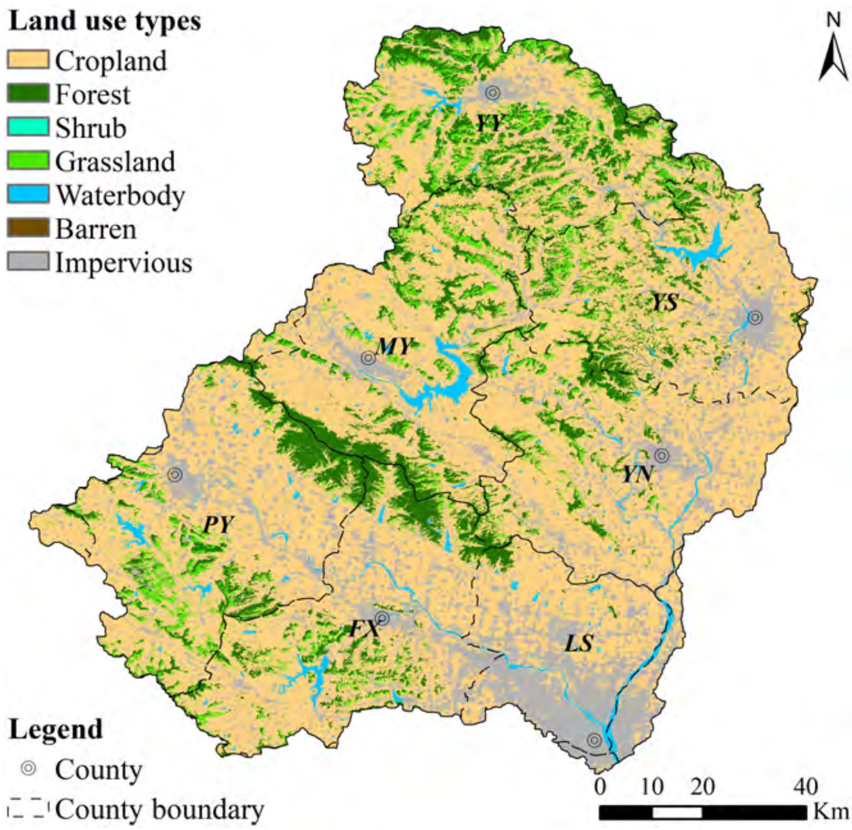

FIGURE 2
Current land use types in the Yihe River Basin (YRB).

methodological approach, as it can effectively capture their long-term temporal dynamics. To quantify the long-term temporal dynamics of NPP, temperature, and precipitation, the non-parametric Sen's slope estimator was employed (Jagadeesh and Agrawal, 2015; Sen, 1968). This method is robust for environmental data analysis, as it is resistant to outliers and does not assume a specific data distribution—common challenges in hydrological and climatic time series (Xu, 2024). The core principle involves calculating the median of all possible pairwise slopes between sequential measurements in the time series. For each pair of time points i and j ($j > i$), the slope was computed as Equation 1:

$$\frac{X_j - X_i}{j - i} \tag{1}$$

Here, x denotes variables of interest (annual total NPP, annual mean NPP, annual mean temperature, or annual precipitation). The median of these slopes, known as Sen's slope (β), indicates both the direction and magnitude of the trend (Equation 2):

$$\beta = \text{Median}\left(\frac{X_j - X_i}{j - i}\right) \; 1 < i < j < n \tag{2}$$

where a positive β value corresponds to an increasing trend, while a negative value indicates a decreasing trend. In addition, the magnitude of β directly quantifies the annual rate of change (e.g., $gC/m^2/a/a$ for NPP, °C/a for temperature, mm/a for precipitation).

This method is widely recognized in hydrometeorological trend studies for its reliability in handling non-normal data and missing values, providing a clearer understanding of long-term environmental changes without being skewed by short-term anomalies or noise.

2.3.2 Correlation analysis

As correlation analysis can measure the relationship between two interested variables, it can to some extent explain the influence of climate change on variation in regional NPP. Therefore, the well-known Pearson correlation coefficient (r) was employed to quantify the linear relationship between NPP and climatic factors (Xu, 2024), investigating the driving mechanisms behind NPP fluctuations. The coefficient r is defined as the product of the covariance between two variables divided by their standard deviations, calculated as Equation 3:

$$r_{xy} = \frac{\sum_{i=1}^{n}\left(X_i - \overline{X}\right)\left(Y_i - \overline{Y}\right)}{\sqrt{\sum_{i=1}^{n}\left(X_i - \overline{X}\right)^2}\sqrt{\sum_{i=1}^{n}\left(Y_i - \overline{Y}\right)^2}} \tag{3}$$

Where the $\bar{x}$ and $\bar{y}$ represent the mean values of NPP and the climatic factor (temperature or precipitation), respectively, and r_{xy} quantifies the degree of their linear correlation (ranging from -1 to $+1$).

The statistical significance of each correlation was tested at $p < 0.05$ to ensure observed relationships were not due to

TABLE 1 Categories and definitions of the correlations between net primary productivity (NPP) and climatic factors.

Categories	*r*	*P*-value
Highly significant positive correlation	$r > 0$	$P < 0.01$
Significant positive correlation		$P < 0.05$
Non-significant positive correlation		$P > 0.05$
Non-significant negative correlation	$r < 0$	$P > 0.05$
Significant negative correlation		$P < 0.05$
Highly significant negative correlation		$P < 0.01$

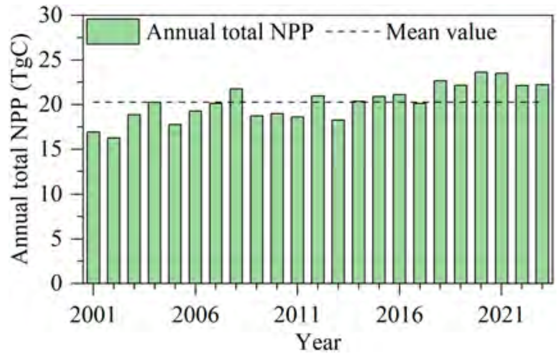

FIGURE 3
Temporal evolution of annual total net primary productivity (NPP) in the Yihe River Basin (YRB) between 2001 and 2023.

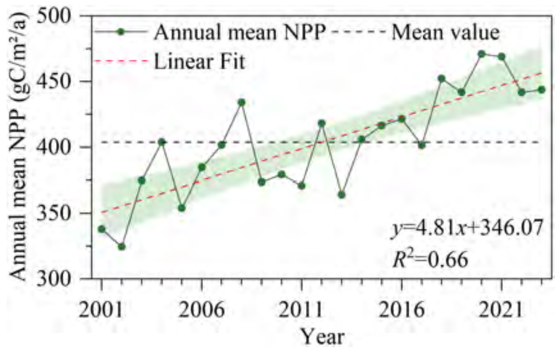

FIGURE 4
Temporal evolution of annual mean net primary productivity (NPP) in the Yihe River Basin (YRB) between 2001 and 2023.

random chance. To facilitate spatial visualization, correlations were categorized into six groups based on the sign of *r* and its statistical significance (Chen et al., 2023; Yang et al., 2021), as presented in Table 1.

3 Results

3.1 Spatiotemporal dynamics of NPP

3.1.1 Temporal evolution of NPP

Statistical results for the annual total and annual mean NPP within the YRB from 2001 to 2023 are presented in Figures 3, 4, respectively. During this time period, the annual total NPP in the basin fluctuated between 16.27 and 23.61 TgC, with a multi-year average of 20.24 TgC. The lowest value occurred in 2002, while the peak was observed in 2020. Temporally, the total annual NPP in 10 years (including 2001–2003, 2005–2006, 2009–2011, 2013, and 2017) fell below the multi-year average, whereas it exceeded the average level in the remaining 13 years (including 2004, 2007–2008, 2012, 2014–2016, and 2018–2023). Overall, the annual total NPP exhibited a fluctuating yet increasing trend, accumulating a net increase of approximately 5.96 TgC over the 23-year period (Figure 3).

The annual mean NPP also exhibited a clear increasing trend with fluctuations (Figure 4). Over the past two decades, the annual mean NPP ranged between 324.65 and 471.11 gC/m^2/a, with a multi-year average of 403.75 gC/m^2/a and a range of 146.46 gC/m^2/a. Moreover, the years in which the highest and lowest annual mean NPP occurred aligned with those for annual total NPP. Specifically, the year 2002 recorded the lowest annual mean NPP, 79.10 gC/m^2/a less than the long-term averages, whereas the highest annual mean NPP in 2020, 67.36 gC/m^2/a more than the long-term averages. The temporal evolution of annual mean NPP in the YRB can be segmented into three stages of significant increase: a continuous increase from 2002 to 2004, during which the annual mean NPP increased from 324.65 to 404.01 gC/m^2/a, a stepwise increase from 2005 to 2008, where the annual mean NPP rose from 353.96 to 434.21 gC/m^2/a, and a fluctuating upward phase from 2009 to 2021, during which the annual mean NPP fluctuated and increased from 364.14 to 471.11 gC/m^2/a. The synchrony trends in both annual total and mean NPP collectively confirm a general improvement in vegetation productivity within the YRB, indicating a progressive recovery of the terrestrial ecosystem.

3.1.2 Spatial distribution of NPP

To clearly investigate the spatial variation for annual mean NPP in the YRB, and referring to the NPP classification standard for temperate basins in China (Ma et al., 2024), the multi-year average of annual mean NPP was categorized into five classes: Low NPP (0–150 gC/m^2/a), Moderately low NPP (150–300 gC/m^2/a), Medium NPP (300–450 gC/m^2/a), Moderately high NPP (450–600 gC/m^2/a), and High NPP (>600 gC/m^2/a).

The spatial distribution of multi-year average annual mean NPP across the YRB displayed significant regional heterogeneity, with higher values in mountainous peripheral areas and lower values in urbanized central zones (Figure 5). Low NPP zones were predominantly located in southern Lanshan District. Medium NPP areas were widely distributed, especially throughout Yishui County, Pingyi County, and central Mengyin County. High NPP values were mainly observed in southern Yiyuan County, eastern Yi'nan County, and northeastern parts of Pingyi and Fei Counties.

To further explore the spatiotemporal dynamics of NPP across the YRB, a comparative assessment of annual mean NPP from five representative years (2001, 2006, 2011, 2016, 2021) was conducted to further explore spatiotemporal dynamics (Figure 6). These years were selected to cover the entire study period and correspond to key

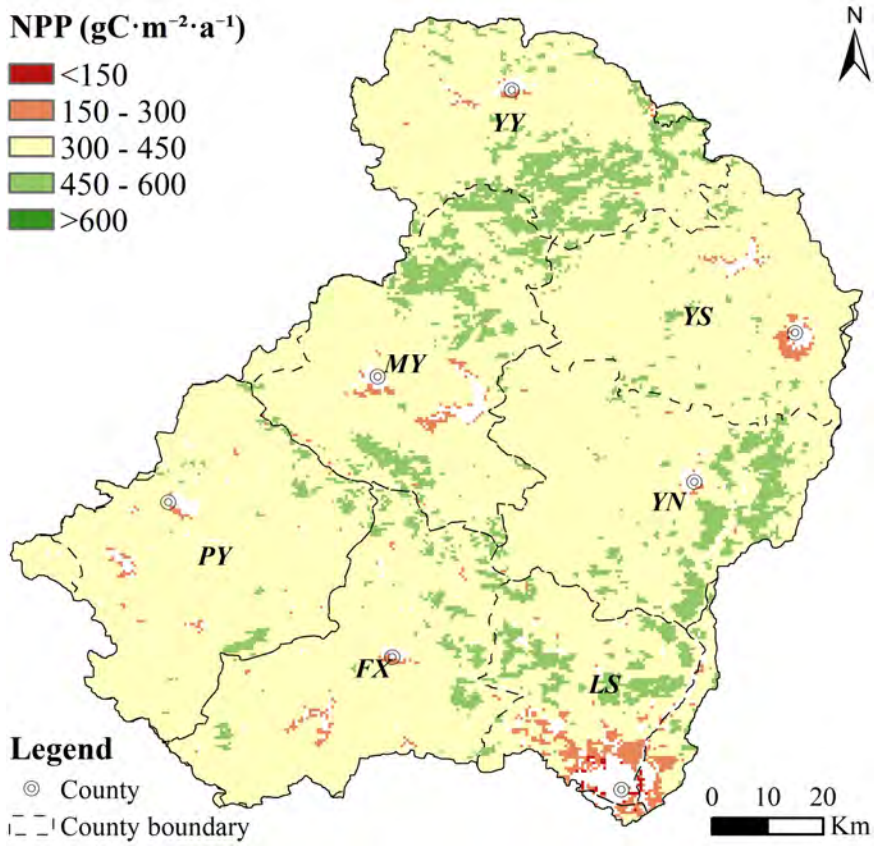

FIGURE 5
Spatial distribution patterns of multi-year average annual mean net primary productivity (NPP) across the Yihe River Basin (YRB) between 2001 and 2023.

stages of ecological projects (e.g., GFGP) in the basin, facilitating analysis of long-term NPP change trends. Between 2001 and 2006, NPP values were mostly concentrated within the medium range, with a noticeable decline in the moderately low category and a marked expansion of moderately high values, particularly in eastern and southern Yi'nan County and central Yiyuan County. From 2006 to 2011, medium-level NPP continued to dominate; however, 2011 was characterized by generally lower productivity, falling below the multi-year average, along with a pronounced reduction in moderately high NPP areas. During 2011–2016, the predominant NPP range shifted to 300–600 $gC/m^2/a$. A substantial transition from medium to moderately high values occurred, especially in Yiyuan County and central Mengyin County. By 2021, a significant increase in NPP was observed, with values largely falling between 450 and 600 $gC/m^2/a$ and a notable expansion of areas exceeding 600 $gC/m^2/a$, sporadically distributed across low mountainous regions at the southern and central parts of the basin. Taken together, despite strong spatial variability throughout the study period, NPP demonstrated an overall increasing trend between 2001 and 2023.

3.1.3 Spatiotemporal trends in NPP

To assess the spatial distribution patterns of interannual variations in NPP, the Sen's slope estimator method was employed in a pixel-scale analysis to quantify interannual trends in NPP across the YRB between 2001 and 2023. As illustrated in Figure 7, the slope range for NPP variation within the entire basin spans from -10.84 to 15.71 $gC/m^2/a/a$, with an average value of 4.75 $gC/m^2/a/a$. Overall, positive slope values were prevalent across most areas, which indicates a widespread increase in NPP and vegetation productivity. The majority of the basin area exhibited positive slope values, suggesting a widespread increasing trend in vegetation productivity.

This widespread enhancement of NPP could be attributed to climate change as well as human activities, representing the combined effects of these factors. Specifically, rising temperatures and increased precipitation have boosted vegetation productivity within terrestrial ecosystems, while ecological conservation measures in the form of afforestation and other vegetation restoration projects have effectively promoted increased vegetation cover and improved ecosystem conditions. In contrast, negative slopes were predominantly observed in southern Lanshan District, eastern parts of Yishui and Yi'nan Counties, northern Yiyuan County, and northeastern Pingyi County. This degradation may be linked to human activities, particularly urban expansion, land development and agricultural intensification, which have led to reduced vegetation cover and increased ecological pressure. In general, the observed significant increase in NPP throughout the basin indicates not only a boost in vegetation productivity but also an improvement in overall ecological health, resulting from the confluence of climatic changes and proactive human management, typically the implementation of ecological restoration projects.

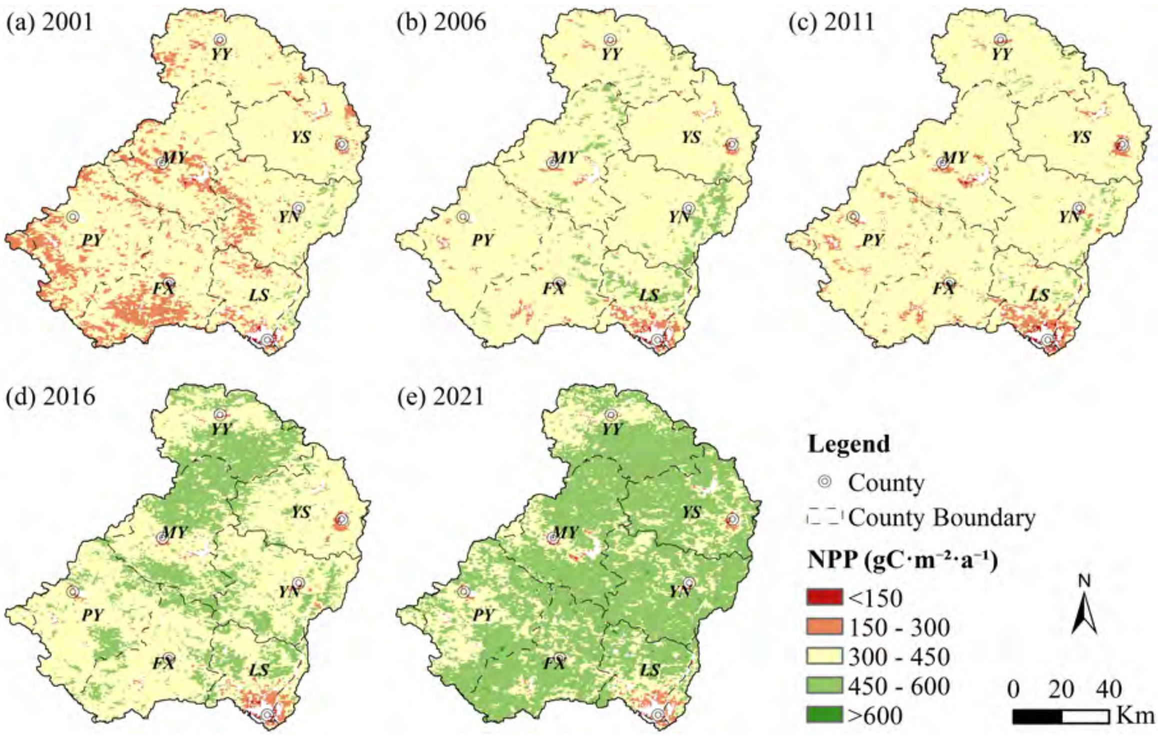

FIGURE 6
Spatial distribution patterns of annual mean net primary productivity (NPP) at five representative years across the Yihe River Basin (YRB).

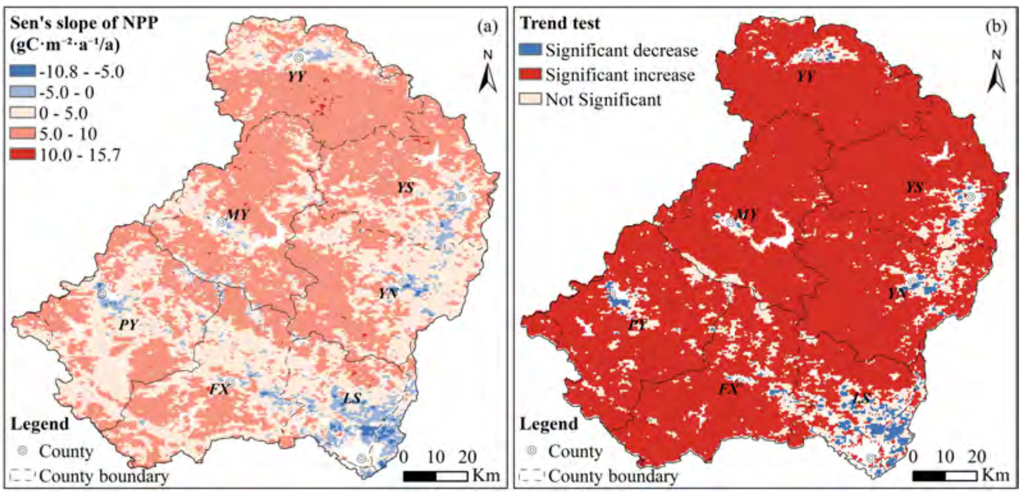

FIGURE 7
Spatial distribution patterns of annual mean net primary productivity (NPP) trends across the Yihe River Basin (YRB) between 2001 and 2023. **(a)** Trend magnitude of the annual mean NPP. **(b)** Trend test of annual mean NPP at 95% confidence level.

3.2 Spatiotemporal variations of climatic factors

3.2.1 Temporal variations of climatic factors

Based on meteorological data analysis, Figure 8 illustrates the interannual variation characteristics of the annual mean temperature and annual precipitation within the YRB. As presented on Figure 8a, the annual mean temperature across the entire basin fluctuates between 12.77 °C and 14.51 °C, at a long-term average of 13.68 °C. Notably, the lowest annual mean temperature recorded was 12.77 °C in 2012, while the highest reached 14.51 °C in 2023. Overall, the annual mean temperature exhibits fluctuating yet statistically significant warming trends, with an annual increase rate of 0.04 °C. Furthermore, the analysis of temperature anomalies (Figure 8c) indicates that the annual mean temperature over the past decade has consistently exceeded the long-term average,

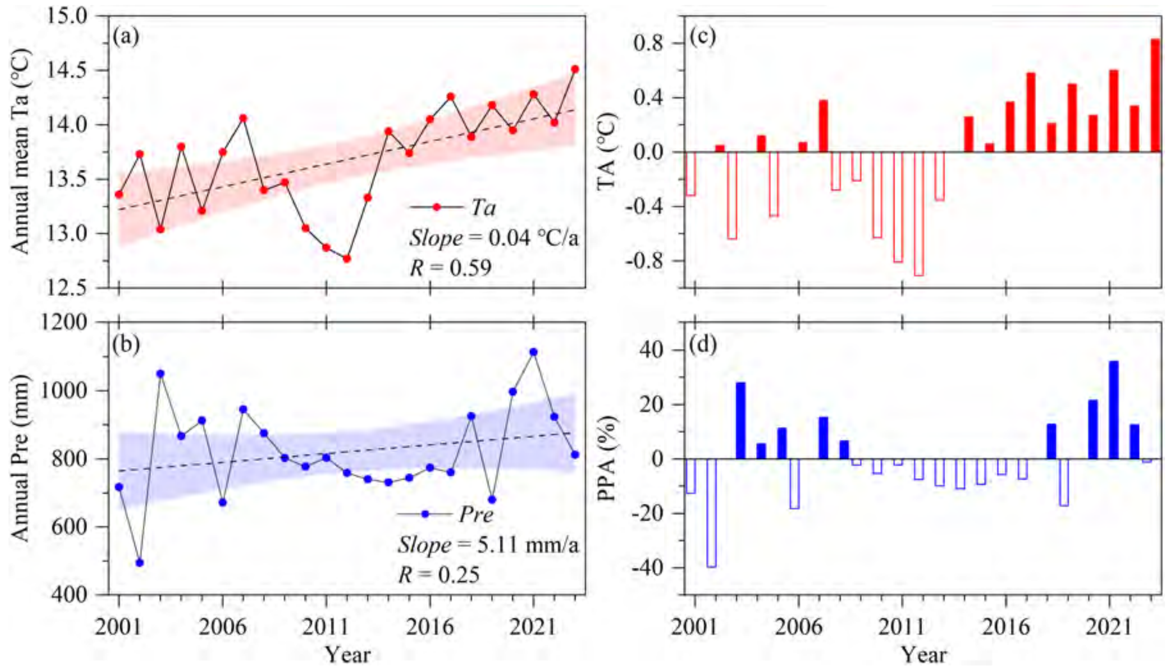

FIGURE 8
Interannual variation and anomalies in annual mean temperature (Ta) and annual precipitation (Pre) in the Yihe River Basin (YRB) between 2001 and 2023. **(a)** Annual mean temperature. **(b)** Annual precipitation. **(c)** Temperature anomalies. **(d)** Percentage of precipitation anomalies.

corroborating a persistent and intensifying warming trend in the YRB.

Different from interannual temperature variations, as depicted by Figure 8b, annual precipitation exhibits significant variability, fluctuating from 495.11 to 1114.76 mm, with a long-term average of 816.6 mm. The year 2002 marked the minimum precipitation at 495.11 mm, whereas 2021 recorded the maximum at 1114.76 mm. The temporal evolution of precipitation can be divided into several distinct stages: a sharp decline occurred between 2003 and 2006, followed by a continued decreasing trend during 2007–2010. The period from 2011 to 2017 was characterized by relative stability with minor fluctuations. A noticeable reduction in precipitation occurred between 2018 and 2019, followed by a steady increase until 2021, and then a pronounced decrease was observed from 2022 to 2023. Despite these fluctuations, the overall trend in precipitation showed only slight variability without a dominant monotonic direction (Figure 8d), reflecting the complex interplay of regional climatic drivers and monsoonal influences. The interannual variation in precipitation stands in sharp contrast to the significant warming trend of annual mean temperature, further highlighting the asynchronous changes in hydrothermal conditions within the basin.

3.2.2 Spatial variations of climatic factors

Based on a pixel-scale spatial analysis for the study period 2001–2023, Figure 9 illustrates the spatial distribution patterns of the mean annual temperature as well as the mean annual precipitation in the YRB during the study period. Overall, the two climatic factors exhibit distinct spatial heterogeneity. As observed in Figure 9a, with the exception of the central Mengshan mountains and its adjacent regions, the multi-year average temperature across the entire basin displays a gradual decrease from southwest toward northeast, with higher temperatures predominantly observed in Pingyi County, Fei County and Lanshan District. In contrast, lower temperatures are predominantly found in northern Yiyuan County, northern Yishui County, and central Mengyin County.

Regarding precipitation, Figure 9b reveals significant spatial heterogeneity in the mean annual precipitation within the basin, exhibiting a general trend of gradual decrease from eastern toward western of the basin, with the Mengshan mountains and its adjacent regions where with higher precipitation due to high altitude. This distribution is influenced by the temperate monsoon climate and topographic factors of the region. The southeastern monsoon carries moist air from the ocean, which encounters the eastern part of the basin first. Here, topographic uplift enhances condensation and rainfall. Conversely, the northwestern areas lie on the leeward side of these monsoon winds, experiencing a rain shadow effect accompanied by föhn winds, which reduce the potential for heavy precipitation. As a result, northwestern sections of the basin receive comparatively less precipitation.

3.3 Patterns of NPP response to climate change

3.3.1 Response of NPP to temperature variations

To clearly quantify the response of NPP to temperature variations between 2001 and 2023 in the YRB, a pixel-based correlation analysis based on Pearson correlation coefficient was conducted. Figure 10a displays the spatial distribution pattern of the correlation coefficient between annual mean NPP and

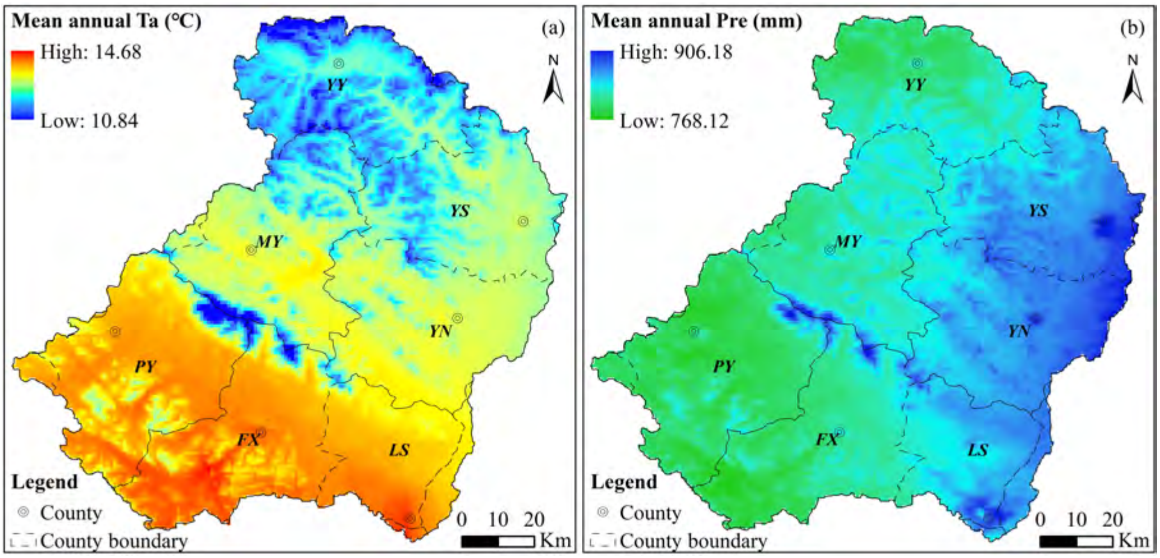

FIGURE 9
Spatial distribution patterns of the two primary climatic factors across the Yihe River Basin (YRB) between 2001 and 2023. **(a)** Mean annual temperature. **(b)** Mean annual precipitation.

temperature, with values in the range of −0.63 to 0.86 and an average of 0.46, indicating an overall weak to moderate positive correlation. Spatially, the NPP in areas accounting for 97% of the basin exhibits a positive correlation with temperature. For clearer interpretation, the significance of the correlation was classified into six levels (Figure 10b). The statistical breakdown reveals that 39% of the basin exhibits an highly significant positive correlation, predominantly located in Pingyi, Fei, Yi'nan, and Yishui counties; 38% shows a significant positive correlation, primarily concentrated in southern Yi'nan and northern Yishui, with some scattered distribution in Pingyi, Fei, and Yi'nan; and 20% demonstrates a non-significant positive correlation, primarily found in northern Yiyuan, southern Yishui, and northern Yi'nan, with minor areas in Pingyi and Mengyin. In contrast, only 3% of the basin displays a negative correlation with temperature, of which 2.3% is non-significantly negative correlation. These areas are spread across Lanshan District, the eastern parts of Yinan and Yishui, the northern part of Pingyi, and certain northern sections of Yiyuan.

3.3.2 Response of NPP to precipitation variations

Similar to temperature, pixel-based correlation analysis was employed to quantify the relationship between precipitation and NPP in the YRB between 2001 and 2023. As presented in Figure 11a, the r between precipitation and NPP varied in the range between −0.28 and 0.84, in which the average value was 0.45. Statistical analysis at the pixel scale revealed that NPP and precipitation are positively correlated across 99.2% of the basin area. Specifically, as illustrated in Figure 11b, a highly significant positive correlation was identified across 25.5% of the total basin area, with its core distribution in Yishui County, extending into the south-central regions of Pingyi County and the northwestern part of Mengyin County. A significant positive correlation constituted 48.3% of the basin, exhibiting a widespread pattern across Pingyi, Yiyuan, Yi'nan, and Yishui counties. Meanwhile, a non-significant positive correlation made up 25.4%, found predominantly in Lanshan District. In contrast, negative correlations were minimal only for 0.8%, located mostly in Lanshan District with sporadic occurrences in Fei, Yi'nan, and Mengyin counties.

4 Discussion

4.1 Spatiotemporal dynamics of NPP and its driving forces

The overall fluctuating increasing trend of NPP in the YRB from 2001 to 2023 aligns with the vegetation recovery trends observed in many regions of China implementing ecological restoration projects, such as the Loess Plateau (Li et al., 2023) and the Yellow River Basin (Chen et al., 2023), reflecting a dual driving mechanism of favorable climatic conditions and localized human interventions. This pattern of increasing NPP is widely observed. For instance, a recent global study of marsh wetlands across diverse climatic zones also reported a significant increasing trend in NPP from 2000 to 2022, particularly in regions like the northern highlands of Brazil and South Africa (Zhang J. et al., 2025). Furthermore, research on global terrestrial ecosystems indicates a clear latitudinal pattern in NPP changes, with mid-to-high latitude temperate and cold-temperate zones (to which the YRB belongs) showing a significant increasing trend, which contrasts with the non-significant or even decreasing trends observed in some tropical and subtropical regions (Xu et al., 2023).

Notably, this temperate zone NPP increase is consistent with findings from Romania's forests, where 99% of forested areas showed positive NPP trends driven by warming temperatures (Prăvălie et al., 2023), though the YRB's monsoon climate adds precipitation as a key co-driver. From the temporal perspective, the increasing trend of NPP is closely related to the overall upward

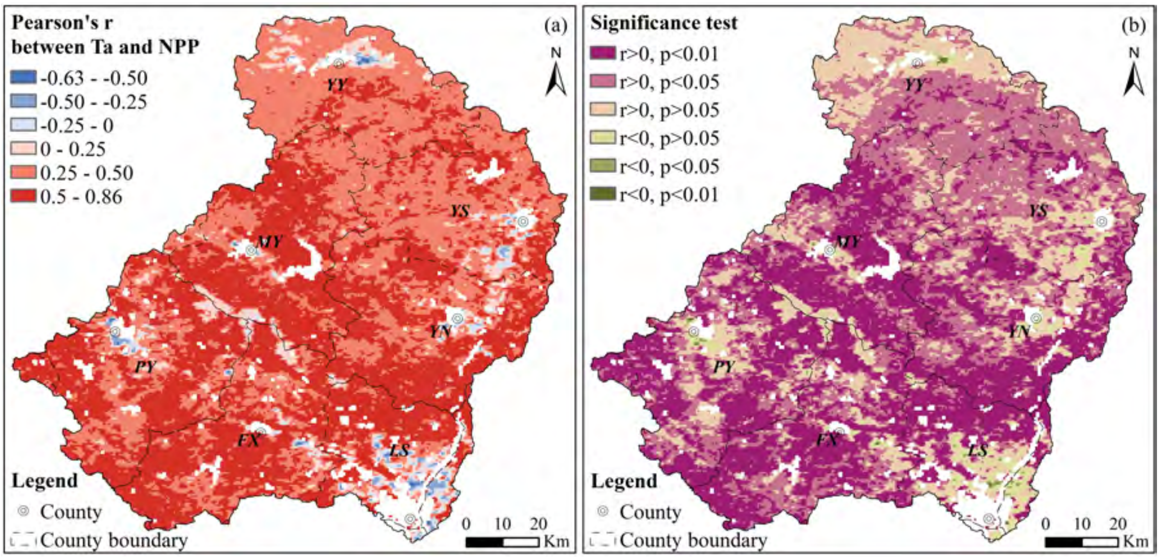

FIGURE 10
Spatial distribution patterns of the correlation and significance between annual mean temperature and net primary productivity (NPP) across the Yihe River Basin (YRB) between 2001 and 2023. **(a)** Pearson correlation coefficients. **(b)** Statistical significance test of the Pearson correlation coefficients with six levels.

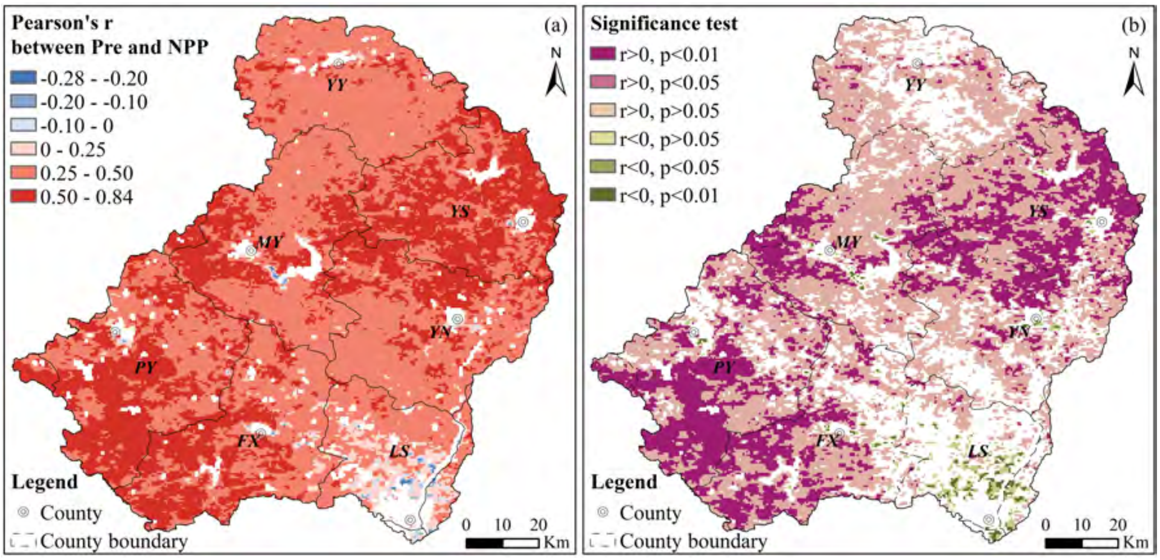

FIGURE 11
Spatial distribution patterns of the correlation and significance between Precipitation and net primary productivity (NPP) across the Yihe River Basin (YRB) between 2001 and 2023. **(a)** Pearson correlation coefficients. **(b)** Statistical significance test of the Pearson correlation coefficients with six levels.

trends of temperature and precipitation in the basin. The annual mean temperature increased at a rate of 0.04 °C/a, and moderate warming extends the vegetation growing season and enhances photosynthetic enzyme activity, while the increasing precipitation alleviates seasonal drought stress that limits vegetation growth. This hydrothermal synergy is distinct from arid regions like northeastern Iran, where NPP is constrained by soil salinity and limited precipitation despite temperature increases (Gholami et al., 2025), highlighting the importance of balanced precipitation in monsoon-influenced basins. Spatially, NPP exhibits a distinct pattern of "higher in mountainous peripheral areas and lower in urbanized central zones," which is jointly regulated by topography, land use types, and human activity intensity. High NPP values are concentrated in hilly and forested areas such as southern Yiyuan County and eastern Yi'nan County, where long-term afforestation initiatives have significantly improved vegetation coverage, a pattern also observed in the Eastern Indian Himalayan region, where progressive land use changes (e.g., degraded forests to agroforestry) enhanced NPP and carbon sequestration (Kurmi et al., 2025). Medium NPP areas are distributed in

10.3389/ffgc.2025.1743125

agricultural plains dominated by wheat-maize rotation systems, with stable productivity supported by sufficient water and fertilizer inputs, similar to the agricultural regions of Pakistan's temperate ecoregions where moderate elevation and adequate precipitation sustain consistent crop productivity (Mehmood et al., 2024). Low NPP zones are mainly located in highly urbanized southern Lanshan District, where extensive impervious surfaces and reduced vegetation coverage lead to low carbon sequestration capacity, which is a common phenomenon in rapidly urbanizing regions globally, such as the Central Plains urban agglomeration where urban expansion directly caused NPP declines of 130.84 gC/m^2/a (Mu et al., 2023) and the Niger River Basin where urbanization and agricultural expansion drove widespread NPP reduction (Chukwuka et al., 2023).

The spatial trend of NPP further confirms the heterogeneous impact of human activities: most areas show a positive increasing trend (average Sen's slope of 4.75 gC/m^2/a), attributed to climate warming, increased precipitation, and ecological restoration projects such as afforestation (Gong et al., 2023). In contrast, negative trends in NPP are concentrated in areas with intense urban expansion and intensive agricultural development, indicating that excessive human disturbance suppresses vegetation productivity (Wu et al., 2014). This is consistent with findings in the western Himalayas, where Sharma et al. (2022) observed a significant decline in NPP in urbanized core areas due to construction land encroaching on forest and cropland, while a slight increasing trend in NPP was observed in remote mountainous areas attributed to temperature rise promoting vegetation growth.

4.2 Mechanisms of climate factors regulating NPP

Correlation analysis confirms that climate factors (temperature and precipitation) play key roles in regulating NPP dynamics in the YRB, with precipitation as the dominant climatic driver, which is consistent with findings from other monsoon climate regions (Yang et al., 2021).

Precipitation is positively correlated with NPP across 99.2% of the basin area, with an average Pearson correlation coefficient of 0.45. The YRB has a typical temperate monsoon climate, with 65%–70% of annual precipitation concentrated in the summer, which is highly synchronized with the peak growing season of vegetation. Sufficient summer precipitation provides abundant soil moisture for photosynthesis, directly promoting biomass accumulation. This precipitation-dominant pattern contrasts with temperature-limited regions such as the Tibetan Plateau (Zheng et al., 2020) and Romania's forests (Prăvălie et al., 2023), where warming is the primary driver of NPP increase, and arid regions like southwestern Australia where reduced precipitation led to significant NPP declines (Brouwers and Coops, 2016). However, localized negative correlations between precipitation and NPP were observed in highly urbanized areas such as Lanshan District. This abnormal phenomenon is mainly due to surface impermeabilization caused by urbanization: a large number of concrete and asphalt surfaces prevent precipitation from infiltrating into the soil, limiting water availability for vegetation roots even with increased precipitation. Additionally, the Urban Heat Island (UHI) Effect intensifies evapotranspiration, exacerbating vegetation moisture stress and offsetting the positive impact of precipitation (Wu et al., 2014), and this is a similar pattern reported in Chinese cities where urban heat islands reduced vegetation productivity despite adequate precipitation (Zhao Y. et al., 2025).

Beyond the positive effects of precipitation, temperature also provides a critical influence, particularly in regulation of spring phenological greening and autumn senescence, with similar findings reported in other temperate monsoon regions (Tang et al., 2024; Yuan et al., 2023). Temperature exhibits an overall weak to moderate positive correlation with NPP, with 97% of the basin showing a positive correlation. For the temperate monsoon climate of the YRB, moderate warming enhances photosynthetic efficiency and extends the growing season, especially in agricultural and forest ecosystems (Liu et al., 2015). Highly significant positive correlations between temperature and NPP are mainly distributed in Pingyi, Fei, Yi'nan, and Yishui counties, where increased temperature in the growing season accelerates crop and tree growth, which consistent with observations in Pakistan's temperate ecoregions where moderate temperature increases promoted vegetation productivity in mid-altitude areas (Mehmood et al., 2024). In contrast, negative correlations are limited to 3% of the basin area, mostly in urbanized regions. The UHI Effect in these areas leads to abnormally high temperatures, inducing stomatal closure in plants to reduce water loss, thereby suppressing photosynthesis and resulting in lower NPP (Zhang et al., 2024), and this is a common mechanism also observed in humid high-productivity cities where extreme urban warming outweighs precipitation benefits (Zhao Y. et al., 2025).

Notably, complex interactions exist between temperature and precipitation: in years with both high temperature and sufficient precipitation, the synergistic effect of hydrothermal conditions maximizes vegetation productivity; however, in years with high temperature and insufficient precipitation, warming exacerbates water stress, leading to reduced NPP. This non-linear interaction reflects the complexity of NPP responses to climate change in the YRB, similar to the interactive effects of temperature and precipitation observed in arid regions like the Chad Lake and Aral Sea basins (Igboeli et al., 2025), where climate variability amplified the impacts of human activities on NPP.

4.3 Impacts of human activities on NPP spatial heterogeneity

Human activities, particularly land use changes associated with afforestation, urbanization, and agricultural development, have exerted complex and spatially heterogeneous impacts on NPP, reflecting the specific socio-economic development context of the basin (Zhang et al., 2024; Ge et al., 2021; Wu et al., 2014).

Afforestation under national ecological restoration projects, such as the GFPP, has significantly promoted NPP increase in mountainous areas of the YRB. Since the 1950s, continuous afforestation initiatives have reversed historical vegetation degradation, and the expansion of forest land has directly enhanced regional carbon sequestration capacity. From 2000 to 2020, the afforestation area in the YRB increased by 6.3% (Yang and Li, 2024), which is consistent with the high NPP values observed in hilly forested areas. This finding aligns with studies on the Loess Plateau, where ecological restoration projects have significantly improved vegetation productivity (Li et al., 2023), and global examples like Pakistan's "Billion Tree Afforestation Project" which drove positive NPP trends in 72.44% of temperate ecoregions (Mehmood et al., 2024). However, the YRB's afforestation success contrasts with south-central Chile, where exotic tree plantation expansion increased NPP but caused ecological fragmentation and biodiversity loss (Martínez et al., 2019), highlighting the importance of prioritizing native species, a strategy also emphasized in the YRB's management recommendations.

Urbanization, in contrast, has a suppressive effect on NPP. Over the past two decades, urban construction land in the YRB increased by 12.5%, while cropland decreased by 8.2% (Yang and Li, 2024). The expansion of impervious surfaces and reduced vegetation coverage in urban areas directly reduce NPP, and the UHI effect further exacerbates thermal and water stress on residual vegetation (Wu et al., 2014). This explains why low NPP zones are concentrated in highly urbanized southern Lanshan District and why negative NPP trends are observed in areas with intense urban expansion. Globally, similar urbanization-driven NPP losses have been reported in the Central Plains urban agglomeration (Mu et al., 2023), the Yangtze River Delta (Wu et al., 2014), and the Niger River Basin (Chukwuka et al., 2023), with direct NPP loss from land conversion ranging from 130 to 247 gC/m/^{2}/a in densely urbanized regions. Notably, the YRB's urban NPP decline is less severe than in megacities like Beijing-Tianjin-Hebei (Zhang et al., 2024) and Changsha-Zhuzhou-Xiangtan (Zhang C. et al., 2025), possibly due to earlier-stage urbanization and relatively more retained green space.

Agricultural activities show a dual impact on NPP. The YRB is an important agricultural production zone, with cropland accounting for over 62% of the basin area (Qiao et al., 2025; Yang and Li, 2024). The stable agricultural management mode (wheat-maize rotation system) and sufficient water and fertilizer input ensure moderate vegetation productivity, making agricultural plains the main distribution area of medium NPP. This aligns with findings from India's agricultural regions, where irrigation and fertilizer use drove NPP increases in northern and northwestern areas (Bejagam and Sharma, 2022). However, intensive agricultural development may lead to soil degradation in the long term, and seasonal crop replacement limits further improvement of NPP compared with forest ecosystems (Chen et al., 2020), a constraint also observed in the Eastern Indian Himalayan region where monoculture plantations had lower NPP than agroforestry systems (Kurmi et al., 2025). Additionally, irrigation measures in agricultural areas can alleviate the negative impact of irregular monsoon rainfall on NPP, which is consistent with findings in other agriculture-dependent monsoon regions (Yang et al., 2021) and arid agricultural zones where irrigation mitigates climate variability impacts (Igboeli et al., 2025).

It should be noted that the impact of human activities on NPP is more complex and difficult to quantify than that of climate factors. While climate drivers exhibit relatively clear linear or non-linear relationships with NPP, human activities involve multifaceted socio-economic processes, policy interventions, and land management practices that often operate at different spatial and temporal scales. This complexity poses challenges for accurately disentangling human versus climate contributions to NPP changes, a limitation that future research should address through more integrated modeling approaches such as residual trend analysis (Ge et al., 2021) geographical detector models (Gholami et al., 2025), which methods successfully applied in global studies to separate anthropogenic and climatic impacts.

4.4 Ecological management strategies and climate adaptation recommendations

Targeted ecological management and climate adaptation strategies for the YRB are developed based on the spatiotemporal dynamics of NPP and its response to climate change. Under future climate scenarios, temperature is projected to continue rising and precipitation is likely to increase further in the region, which will exacerbate the impacts of climate change on NPP dynamics. Given that human activities such as urbanization have slowed and ecological restoration projects have reached a stable phase in the basin, climate change will become an increasingly dominant factor influencing vegetation productivity, and this trend also predicted for global temperate regions (Huang et al., 2024).

Given the dominant role of precipitation in NPP regulation, water resource management should be optimized: scientific reservoir operation (e.g., Bashan Dam and Andi Dam) and spring irrigation systems should be implemented to alleviate drought stress in agricultural areas, particularly in the western rain shadow region where precipitation is relatively low. This strategy is consistent with water management practices in arid and semi-arid basins like the Niger River Basin (Chukwuka et al., 2023) and the Aral Sea Basin (Igboeli et al., 2025), where improved water allocation mitigated NPP losses from climate variability. For the Urbanization Control Zone (southern Lanshan District, eastern Yishui and Yi'nan Counties), sponge city projects and urban green space expansion are recommended, with priority given to drought-resistant and heat-tolerant native plant species to reduce impervious surfaces, mitigate the UHI Effect, enhance rainwater infiltration, and thus promote NPP recovery in urban areas. Similar urban greening strategies have been effective in reducing NPP losses in Chinese cities (Zhao H. et al., 2025) and the western Himalayas (Sharma et al., 2022), where native species outperformed exotic plants in adapting to urban microclimates. The Mountain Ecological Restoration Zone (southern Yiyuan, eastern Yi'nan, northeastern Pingyi and Fei Counties) should continue afforestation initiatives while prioritizing native tree species to improve ecosystem stability and avoid excessive water consumption, ensuring the sustainability of carbon sink capacity without exacerbating water stress in dry years. This can a lesson learned from south-central Chile where exotic plantations caused long-term ecological degradation (Martínez et al., 2019), thus ensuring the sustainability of carbon sink capacity without exacerbating water stress in dry years. In the Agricultural Stability Zone, water-saving irrigation technologies (e.g., drip irrigation) and adaptive crop rotation systems aligned with precipitation patterns should be promoted to balance agricultural productivity and ecological protection, reducing the vulnerability of NPP to monsoon variability. This approach is supported by successful practices in Pakistan's temperate agricultural regions

(Mehmood et al., 2024) and the Eastern Indian Himalayas (Kurmi et al., 2025), where diversified cropping systems enhanced NPP and carbon sequestration. These strategies integrate the dual influences of climate change and human activities, providing actionable guidance for enhancing the YRB's ecosystem resilience and supporting sustainable development in warm temperate monsoon medium-sized basins worldwide.

4.5 Research limitations and future directions

Despite the robust methodology and datasets used, this study has certain limitations that need to be addressed in future research. The MOD17A3HGF product may still contain uncertainties related to cloud cover during the monsoon season and the algorithm's ability to capture rapid vegetation changes (Running et al., 2004). Future studies could integrate ground-based observations and employ advanced methods such as the CASA model optimized for monsoon climate parameters to improve the accuracy of NPP estimation (Cai et al., 2025; Wang F. et al., 2025; Ma et al., 2023; Yang et al., 2021; Liu et al., 2015) or machine learning-based NPP estimation (Prăvălie et al., 2023; Yi and Wu, 2023) to improve the accuracy of NPP estimation.

In addition, this study mainly focused on temperature and precipitation, while other factors such as soil properties, solar radiation, and the CO_2 fertilization effect were not considered. For instance, Hu et al. (2024) estimated that the CO_2 fertilization effect accounts for approximately 32% of the global NPP increase, and future research should incorporate these factors to comprehensively reveal the driving mechanism of NPP dynamics, a gap also highlighted in global NPP studies (Huang et al., 2024). Additionally, the impact of extreme climate events (such as extreme precipitation and heatwaves) on NPP was not analyzed in depth. Given the pronounced seasonality of precipitation in the YRB and the increasing frequency of extreme climate events under global change, future research should focus on the response of NPP to extreme events to improve the climate adaptation capacity of the basin (IPCC, 2021), a priority also identified in studies of Mediterranean climate regions (Brouwers and Coops, 2016) and arid basins (Igboeli et al., 2025).

Moreover, this study did not quantitatively separate the relative contributions of climate change and human activities to NPP variations. While human activities were discussed qualitatively, their specific contribution weights remain unclear. Future studies should apply attribution analysis methods such as residual trend analysis (Ge et al., 2021) or geographical detector models (Gholami et al., 2025) to disentangle the individual and interactive effects of climate and human drivers, providing a clearer scientific basis for targeted management interventions.

5 Conclusion

This study quantified the spatiotemporal dynamics of NPP in the YRB from 2001 to 2023 using MOD17A3HGF data and meteorological reanalysis datasets, employing Sen's slope estimator and Pearson correlation analysis to clarify trends and climate responses. The key findings are: (1) NPP exhibited an overall fluctuating increasing trend, with annual total NPP averaging 20.24 TgC and annual mean NPP averaging 403.75 $gC/m^2/a$, segmented into three significant growth stages; (2) Spatially, NPP was heterogeneous–high in mountainous peripheries, low in urban centers; (3) Both temperature and precipitation showed upward trends, with precipitation as the primary climatic factor positively correlated with NPP, while temperature exhibited weak positive correlations and negative correlations concentrated in urban areas; (4) Human activities shaped spatial heterogeneity, with three management zones (Urbanization Control, Agricultural Stability, Mountain Ecological Restoration) identified to guide targeted action. This study clarifies the response mechanism of NPP to climate change, and provides scientific support for regional ecological restoration and climate adaptation.

Data availability statement

The datasets presented in this study can be found in online repositories. The names of the repository/repositories and accession number(s) can be found below: https://doi.org/10.11888/Meteoro.tpdc.270961 and https://doi.org/10.5281/zenodo.3114194.

Author contributions

HL: Writing – original draft. JX: Writing – review & editing. CN: Writing – review & editing. XY: Writing – review & editing.

Funding

The author(s) declared that financial support was received for this work and/or its publication. This research was funded by the National Natural Sciences Foundation of China (42401152), the Shandong Provincial Natural Science Foundation (ZR2024QD194), and the Doctoral Natural Sciences Foundation of Linyi University (Z6124004).

Conflict of interest

The author(s) declared that this work was conducted in the absence of any commercial or financial relationships that could be construed as a potential conflict of interest.

Generative AI statement

The author(s) declared that generative AI was not used in the creation of this manuscript.

Any alternative text (alt text) provided alongside figures in this article has been generated by Frontiers with the support of artificial intelligence and reasonable efforts have been made to ensure accuracy, including review by the authors wherever possible. If you identify any issues, please contact us.

Publisher's note

All claims expressed in this article are solely those of the authors and do not necessarily represent those of their affiliated organizations, or those of the publisher, the editors and the reviewers. Any product that may be evaluated in this article, or claim that may be made by its manufacturer, is not guaranteed or endorsed by the publisher.

References

Bejagam, V., and Sharma, A. (2022). Impact of climatic changes and anthropogenic activities on ecosystem net primary productivity in India during 2001–2019. *Ecol. Inform.* 70:101732. doi: 10.1016/j.ecoinf.2022.101732

Brouwers, N. C., and Coops, N. C. (2016). Decreasing net primary production in forest and shrub vegetation across southwest Australia. *Ecol. Indicat.* 66, 10–19. doi: 10.1016/j.ecolind.2016.01.010

Cai, D., Dang, X., Zhao, S., and Qiu, F. (2025). Spatiotemporal variation and driving mechanisms of grassland NPP in farming-pastoral ecotone of the Loess Plateau from 1990 to 2020. *Res. Soil Water Conserv.* 32, 236–244. doi: 10.13869/j.cnki.rswc.2025.06.024

Chen, Y., Chen, L., Cheng, Y., Ju, W., Chen, H. Y. H., and Ruan, H. (2020). Afforestation promotes the enhancement of forest LAI and NPP in China. *For. Ecol. Manag.* 462:117990. doi: 10.1016/j.foreco.2020.117990

Chen, Y., Guo, D., Cao, W., and Li, Y. (2023). Changes in net primary productivity and factor detection in China's Yellow River basin from 2000 to 2019. *Remote Sens.* 15:2798. doi: 10.3390/rs15112798

Chukwuka, O., Emeka, I., Ibrahim, Y., Fenetahun, Y., Yuan, Y., and Yongdong, W. (2023). Remote sensing approach in evaluating anthropogenic impacts on the spatiotemporal changes in net primary productivity of the Niger river basin, from 2000 to 2020. *Heliyon* 9:e21246. doi: 10.1016/j.heliyon.2023.e21246

Cong, S., Ding, X., Chang, W., Wang, Y., Yu, H., and Huang, J. (2025). Response of net primary productivity of vegetation to drought change in the arid zone of central Ningxia. *Bull. Soil Water Conserv.* 45, 1–11. doi: 10.13961/j.cnki.stbctb.2025.04.005

Du, T., Yang, F., Li, J., Zhang, C., Cui, K., and Zheng, J. (2025). Long time series spatiotemporal variations in NPP based on the CASA model in the eco-urban agglomeration around poyang lake. China. *Remote Sens.* 17:80. doi: 10.3390/rs17010080

FAO (2023). *State of the world's soil resources 2023: Soil biodiversity for sustainable development*. Rome: Food and Agriculture Organization of the United Nations.

Field, C. B., Behrenfeld, M. J., Randerson, J. T., and Falkowski, P. (1998). Primary production of the biosphere: Integrating terrestrial and oceanic components. *Science* 281, 237–240. doi: 10.1126/science.281.5374.237

Gang, C., Zhang, Y., Wang, Z., Chen, Y., Yang, Y., Li, J., et al. (2017). Modeling the dynamics of distribution, extent, and NPP of global terrestrial ecosystems in response to future climate change. *Global Plan. Change* 148, 153–165. doi: 10.1016/j.gloplacha.2016.12.007

Ge, W., Deng, L., Wang, F., and Han, J. (2021). Quantifying the contributions of human activities and climate change to vegetation net primary productivity dynamics in China from 2001 to 2016. *Sci. Total Environ.* 773:145648. doi: 10.1016/j.scitotenv.2021.145648

Gholami, M., Akbari, M., Mahmoudabadi, E., Kazemzadeh, M., and Noughani, M. A. (2025). Analyzing the impacts of natural and anthropogenic drivers on the spatio-temporal changes of net primary production in northeastern Iran. *Anthropocene* 52:100502. doi: 10.1016/j.ancene.2025.100502

Gong, H., Cao, L., Duan, Y., Jiao, F., Xu, X., Zhang, M., et al. (2023). Multiple effects of climate changes and human activities on NPP increase in the three-north shelter forest program area. *For. Ecol. Manag.* 529:120732. doi: 10.1016/j.foreco.2022.120732

Gu, B., Xu, G., Wang, Z., Li, Q., Zhang, Y., and Chen, A. (2025). Quantitative analysis of the spatiotemporal differentiation pattern of vegetation net primary productivity and its multiple driving forces in the Shaanxi section of the Qinling Mountains. *Aeta Eeal. Sin.* 45, 1–13. doi: 10.20103/j.stxb.202504210946

Han, H., Ta, Z., Chen, C., Zhao, T., and Li, P. (2024). Analysis on the spatio-temporal variation and influencing factors of net primary productivity of vegetation in the ecological region of the Yellow River basin from 2001 to 2022. *Environ. Ecol.* 6, 56–67. doi: 10.3969/j.issn.2096-6830.2024.10.08

Hu, X., Feng, H., Tang, Y., Wang, S., Wang, S., Wang, W., et al. (2024). Detection of the contribution of vegetation change to global net primary productivity: A satellite perspective. *Remote Sens.* 16:4692. doi: 10.3390/rs16244692

Huang, H., Rodriguez-Iturbe, I., and Calabrese, S. (2024). Widespread temporal and spatial variability in net ecosystem productivity under climate change. *One Earth* 7, 473–482. doi: 10.1016/j.oneear.2024.01.008

Igboeli, E. E., Chukwuka, O., Ochege, F. U., Onyekwelu, C. A., Ling, Q., Ajaero, C., et al. (2025). Combined impacts of land change and climate variability on ecosystem net primary productivity in arid regions. *Global Plan. Change* 245:104682. doi: 10.1016/j.gloplacha.2024.104682

IPCC (2021). *Climate change 2021: The physical science basis. contribution of working Group I to the Sixth assessment report of the intergovernmental panel on climate changel*. Cambridge: Cambridge University Press.

IPCC (2022). *Climate change 2022: Mitigation of climate change (working Group III contribution to the Sixth assessment report)*. Cambridge: Cambridge University Press.

Jagadeesh, P., and Agrawal, S. (2015). Investigation of trends and its magnitude by non-parameteric Mann-Kendall and Sen's slope methods. *Intern. J. Hydrol. Sci. Technol.* 5, 83–94. doi: 10.1504/IJHST.2015.069281

Kurmi, B., Nath, A. J., Sileshi, G. W., Pandey, R., and Das, A. K. (2025). Land use change affects net ecosystem production in the Eastern Indian Himalayan region. *Environ. Sustainabil. Indicat.* 26:100670. doi: 10.1016/j.indic.2025.100670

LBS (2024). *Linyi statistical yearbook*. China: Linyi Bureau of Statistics.

Li, W., Zhou, J., Xu, Z., Liang, Y., Shi, J., and Zhao, X. (2023). Climate impact greater on vegetation NPP but human enhance benefits after the grain for green program in loess plateau. *Ecol. Indicat.* 157:111201. doi: 10.1016/j.ecolind.2023.111201

Li, Y. (2025). *Distribution, source analysis and environmental-health risk assessment of heavy metals in agricultural soils of the Yihe River Basin*. China: Jinan, Shandong Normal University.

Liang, Y., Zhao, H., Yuan, Z., Wei, D., and Wang, X. (2024). Ecological restoration projects adapt response of net primary productivity of alpine grasslands to climate change across the tibetan plateau. *Remote Sens.* 16:4444. doi: 10.3390/rs16234444

Lin, C., and Dugarsuren, N. (2015). Deriving the spatiotemporal npp pattern in terrestrial ecosystems of mongolia using MODIS imagery. *Photogrammetric Eng. Remote Sens.* 81, 587–598. doi: 10.14358/PERS.81.7.587

Liu, C., Dong, X., and Liu, Y. (2015). Changes of NPP and their relationship to climate factors based on the transformation of different scales in Gansu, China. *Catena* 125, 190–199. doi: 10.1016/j.catena.2014.10.027

Liu, J. (2020). *Runoff and sediment variations and its response to climate and land use in Yihe River Basin*. China: Jinan, Shandong Normal University.

Liu, Z., Liu, C., Wang, H., and Xu, J. (2025). Analysis of spatiotemporal variation characteristics and driving factors of vegetation NPP in Yunnan. *J. Central South Univ. For. Technol.* 45, 144–155. doi: 10.14067/j.cnki.1673-923x.2025.07.015

Long, B., Zeng, C., Zhou, T., Yang, Z., Rao, F., Li, J., et al. (2024). Quantifying the relative importance of influencing factors on NPP in hengduan mountains of the tibetan plateau from 2002 to 2021: A dominance analysis. *Ecol. Inform.* 81:102636. doi: 10.1016/j.ecoinf.2024.102636

Ma, B., Jing, J., Liu, B., Wang, Y., and He, H. (2023). Assessing the contribution of human activities and climate change to the dynamics of NPP in ecologically fragile regions. *Global Ecol. Conserv.* 42:e02393. doi: 10.1016/j.gecco.2023.e02393

Ma, Y., Gao, Z., Wu, Y., Wu, D., Gao, Y., and Xu, X. (2024). Spatial and temporal evolution of NPP and its relationship with temperature and precipitation in jilin province from 2000 to 2020. *Meteorol. Environ. Sci.* 47, 65–74. doi: 10.16765/j.cnki.1673-7148.2024.06.008

Martínez, Y. M., Coll, D. G., Aguayo, M., and Casas-Ledón, Y. (2019). Effects of landcover changes on net primary production (NPP)-based exergy in south-central of Chile. *Appl. Geography* 113:102101. doi: 10.1016/j.apgeog.2019.102101

Mehmood, K., Anees, S. A., Rehman, A., Rehman, N. U., Muhammad, S., Shahzad, F., et al. (2024). Assessment of climatic influences on net primary productivity along elevation gradients in temperate ecoregions. *Trees For. People* 18:100657. doi: 10.1016/j.tfp.2024.100657

Mu, W., Zhu, X., Ma, W., Han, Y., Huang, H., and Huang, X. (2023). Impact assessment of urbanization on vegetation net primary productivity: A case study of the core development area in central plains urban agglomeration, China. *Environ. Res.* 229:115995. doi: 10.1016/j.envres.2023.115995

Pachavo, G., and Murwira, A. (2014). Remote sensing net primary productivity (NPP) estimation with the aid of GIS modelled shortwave radiation (SWR) in a Southern African Savanna. *Intern. J. Appl. Earth Observ. Geoinform.* 30, 217–226. doi: 10.1016/j.jag.2014.02.007

Peng, S. (2019). *1-km monthly mean temperature dataset for china (1901-2024)*. China: National Tibetan Plateau/Third Pole Environment Data Center.

Peng, S. (2020). *1-km monthly precipitation dataset for China (1901-2024)*. China: National Tibetan Plateau/Third Pole Environment Data Center.

Peng, S., Ding, Y., Liu, W., and Li, Z. (2019). 1 km monthly temperature and precipitation dataset for China from 1901 to 2017. *Earth Syst. Sci. Data* 11, 1931–1946. doi: 10.5194/essd-11-1931-2019

Prăvălie, R., Niculiţă, M., Roşca, B., Marin, G., Dumitraşcu, M., Patriche, C., et al. (2023). Machine learning-based prediction and assessment of recent dynamics of forest net primary productivity in Romania. *J. Environ. Manag.* 334:117513. doi: 10.1016/j.jenvman.2023.117513

Qiao, X., Li, Z., Lin, J., and Yang, S. (2025). Traiectory analysis and scenario simulation of land use change in the Yihe River Basin. *J. Shaanxi Normal Univ.* 53, 13–25. doi: 10.15983/j.cnki.jsnu.2025103

Qiao, X., Li, Z., Lin, J., Wang, H., Zheng, S., and Yang, S. (2024). Assessing current and future soil erosion under changing land use based on InVEST and FLUS models in the Yihe River Basin, North China. *Intern. Soil Water Conserv. Res.* 12, 298–312. doi: 10.1016/j.iswcr.2023.07.001

Running, S. W., Nemani, R. R., Heinsch, F. A., Zhao, M., Reeves, M., and Hashimoto, H. (2004). A continuous satellite-derived measure of global terrestrial primary production. *BioScience* 54, 547–560. doi: 10.1641/0006-35682004054[0547:ACSMOG]2.0.CO;2

Running, S., and Zhao, M. (2019). *MOD17A3HGF MODIS/Terra net primary production gap-filled yearly L4 global 500 m SIN grid V006*. South Dakota: NASA Land Processes Distributed Active Archive Center.

Sen, P. K. (1968). Estimates of the regression coefficient based on kendall's tau. *J. Am. Statist. Assoc.* 63, 1379–1389. doi: 10.2307/2285891

Sharma, S., Joshi, P. K., and Fürst, C. (2022). Unravelling net primary productivity dynamics under urbanization and climate change in the western Himalaya. *Ecol. Indicat.* 144:109508. doi: 10.1016/j.ecolind.2022.109508

Song, X., Zhou, Z., Shen, R., Xu, L., Hu, F., Xie, Z., et al. (2025). Evaluating the suitability of NPP simulation for subtropical forest ecosystems by calibrating the Biome-BGC model: An empirical study at interannual and inter-monthly scales. *Ecol. Modell.* 509:111275. doi: 10.1016/j.ecolmodel.2025.111275

Tang, Z., Zhang, Y., Lei, M., Li, Z., Zhao, G., Chen, Y., et al. (2024). Climate-Driven effects on NPP in the tibetan plateau alpine grasslands diminish with increasing elevation. *Remote Sens.* 16:4754. doi: 10.3390/rs16244754

Tum, M., Zeidler, J. N., Günther, K. P., and Esch, T. (2016). Global NPP and straw bioenergy trends for 2000–2014. *Biomass Bioenergy* 90, 230–236. doi: 10.1016/j.biombioe.2016.03.040

Wang, F., Zhang, Z., Du, M., Lu, J., and Chen, X. (2025). Drought amplifies the suppressive effect of afforestation on net primary productivity in semi-arid ecosystems: A case study of the Yellow River Basin. *Remote Sens.* 17:2100. doi: 10.3390/rs17122100

Wang, W., Wang, Y., Zhai, S., Xia, H., Wang, D., and Song, H. (2024). Climate change driven by LUCC reduced NPP in the Yellow River Basin, China. *Global Plan. Change* 242:104586. doi: 10.1016/j.gloplacha.2024.104586

Wang, Y., Tong, X., Li, J., Yang, M., and Wang, Y. (2025). Impacts of climate change and human activities on vegetation productivity in China. *Remote Sens.* 17:1724. doi: 10.3390/rs17101724

Wang, Z., Dong, C., Dai, L., Wang, R., Liang, Q., He, L., et al. (2023). Spatiotemporal evolution and attribution analysis of grassland NPP in the Yellow River source region, China. *Ecol. Inform.* 76:102135. doi: 10.1016/j.ecoinf.2023.102135

Wu, S., Zhou, S., Chen, D., Wei, Z., Dai, L., and Li, X. (2014). Determining the contributions of urbanisation and climate change to NPP variations over the last decade in the Yangtze River Delta. China. *Sci. Total Environ.* 472, 397–406. doi: 10.1016/j.scitotenv.2013.10.128

Xi, Z., Chen, G., Xing, Y., Xu, H., Tian, Z., Ma, Y., et al. (2023). Spatial and temporal variation of vegetation NPP and analysis of influencing factors in Heilongjiang Province, China. *Ecol. Indicat.* 154:110798. doi: 10.1016/j.ecolind.2023.110798

Xu, J. (2024). *Quantitative geography*. Beijing: Higher Education Press.

Xu, X., Luo, Y., Yang, S., Lu, X., Zhou, Q., Liu, M., et al. (2023). Change trend and sustainability of vegetation net primary productivity of terrestrial ecosystems in different global climatic zones. *Acta Ecol. Sin.* 43, 3729–3743. doi: 10.5846/stxb202205061255

Xu, Y., Lu, Y. G., Zou, B., Xu, M., and Feng, Y. X. (2024). Unraveling the enigma of NPP variation in Chinese vegetation ecosystems: The interplay of climate change and land use change. *Sci. Total Environ.* 912:169023. doi: 10.1016/j.scitotenv.2023.169023

Xue, H., Chen, Y., Dong, G., and Li, J. (2023). Quantitative analysis of spatiotemporal changes and driving forces of vegetation net primary productivity (NPP) in the Qimeng region of Inner Mongolia. *Ecol. Indicat.* 154:110610. doi: 10.1016/j.ecolind.2023.110610

Yan, H., Zhan, J., Jiang, Q. O., Yuan, Y., and Li, Z. (2015). Multilevel modeling of NPP change and impacts of water resources in the Lower Heihe River Basin. *Phys. Chem. Earth Parts A/B/C* 7, 29–39. doi: 10.1016/j.pce.2014.12.001

Yan, H., Zhan, J., Yang, H., Zhang, F., Wang, G., and He, W. (2016). Long time-series spatiotemporal variations of NPP and water use efficiency in the lower Heihe River Basin with serious water scarcity. *Phys. Chem. Earth Parts A/B/C* 96, 41–49. doi: 10.1016/j.pce.2016.06.003

Yang, H., Mu, S., and Li, J. (2014). Effects of ecological restoration projects on land use and land cover change and its influences on territorial NPP in Xinjiang, China. *Catena* 115, 85–95. doi: 10.1016/j.catena.2013.11.020

Yang, H., Zhong, X., Deng, S., and Xu, H. (2021). Assessment of the impact of LUCC on NPP and its influencing factors in the Yangtze River basin, China. *Catena* 206:105542. doi: 10.1016/j.catena.2021.105542

Yang, S., and Li, Z. (2024). Spatio-temporal pattern of ecosystem service value evolution in the Yihe River basin in the context of land use change. *Environ. Sci.* 45, 4722–4732. doi: 10.13227/j.hjkx.202307230

Yi, Z., and Wu, L. (2023). Identification of factors influencing net primary productivity of terrestrial ecosystems based on interpretable machine learning – evidence from the county-level administrative districts in China. *J. Environ. Manag.* 326:116798. doi: 10.1016/j.jenvman.2022.116798

Yuan, X., Guo, B., and Lu, M. (2023). The responses of vegetation NPP dynamics to the influences of climate–human factors on qinghai–tibet plateau from 2000 to 2020. *Remote Sens.* 15:2419. doi: 10.3390/rs15092419

Zhang, C., Xiang, G., Sun, H., Zang, Z., and Zhang, M. (2025). Evaluating the impact of urban expansion on ecosystem carbon based on a long time series 30 m resolution NPP dataset. *Ecol. Indicat.* 180:114343. doi: 10.1016/j.ecolind.2025.114343

Zhang, J., Wang, J., Chen, Y., Huang, S., and Liang, B. (2024). Spatiotemporal variation and prediction of NPP in Beijing-Tianjin-Hebei region by coupling PLUS and CASA models. *Ecol. Inform.* 81:102620. doi: 10.1016/j.ecoinf.2024.102620

Zhang, J., Zhao, M., Ma, R., Feng, M., Ding, C., Wu, L., et al. (2025). Different impacts of temperature and precipitation on vegetation net primary production of global marsh wetlands. *Global Plan. Change* 252:104893. doi: 10.1016/j.gloplacha.2025.104893

Zhao, H., Cui, Y., Li, M., Kang, X., Li, W. C., Han, Y. J., et al. (2025). Impacts of climate change and human activities on net primary productivity of vegetation in Ningxia, Northwest China. *Chin. J. Appl. Ecol.* 36, 2429–2441. doi: 10.13287/j.1001-9332.202508.029

Zhao, Y., Chen, H., Ge, W., Shi, S., Li, R., Sinore, T., et al. (2025). Examining the direct and indirect impacts of urbanization on vegetation net primary productivity across Chinese cities. *Agricult. For. Meteorol.* 374:110815. doi: 10.1016/j.agrformet.2025.110815

Zheng, Z., Zhu, W., and Zhang, Y. (2020). Seasonally and spatially varied controls of climatic factors on net primary productivity in alpine grasslands on the tibetan plateau. *Global Ecol. Conserv.* 21:e00814. doi: 10.1016/j.gecco.2019.e00814

Zhou, L., Dong, Q., Pan, Y. J., Yang, F., He, M. L., Huang, X., et al. (2025). Spatiotemporal variations and driving forces of regional-scale NPP based on a multi-method integration: A case study in the Beibu Gulf Economic Zone. *Ecol. Indicat.* 174:113453. doi: 10.1016/j.ecolind.2025.113453

Zhu, P., Liu, G., and He, J. (2023). Spatio-temporal variation and impacting factors of NPP from 2001 to 2020 in Sanjiangyuan region, China: A deep neural network-based quantitative estimation approach. *Ecol. Inform.* 78:102345. doi: 10.1016/j.ecoinf.2023.102345